International Journal of Architectural, Civil and Construction Sciences
ISSN: 2415-1734
Vol:12, No:2, 2018

Bi-Directional Evolutionary Topology Optimization Based on Critical Fatigue Constraint

Khodamorad Nabaki, Jianhu Shen, Xiaodong Huang

***Abstract*—**This paper develops a method for considering the critical fatigue stress as a constraint in the Bi-directional Evolutionary Structural Optimization (BESO) method. Our aim is to reach an optimal design in which high cycle fatigue failure does not occur for a specific life time. The critical fatigue stress is calculated based on modified Goodman criteria and used as a stress constraint in our topology optimization problem. Since fatigue generally does not occur for compressive stresses, we use the p-norm approach of the stress measurement that considers the highest tensile principal stress in each point as stress measure to calculate the sensitivity numbers. The BESO method has been extended to minimize volume an object subjected to the critical fatigue stress constraint. The optimization results are compared with the results from the compliance minimization problem which shows clearly the merits of our newly developed approach.

***Keywords*—**Topology optimization, BESO method, p-norm, fatigue constraint.

I. Introduction

In this research, we have applied the fatigue life as a constraint in our topology optimization problem to reach the optimal design which can withstand a specific life time without fatigue failure. Applying fatigue constraint in topology optimization is considered as one of the difficult engineering problems due to nonlinearity nature of the constraint. There are few researches that consider fatigue life as a constraint in topology optimization, however, all of them have used Solid Isotropic Material with Penalization (SIMP) [1], along with the Method of Moving Asymptotes (MMA) [2] to obtain the optimal design; for example see [3]-[8], among others. So far, there is no report on fatigue-based topology optimization by using the BESO method where discrete 0/1 design variables have been used.

One of the critical comments in the original ESO/BESO methods is that the procedure cannot be easily extended to other constraints, or multi-constraints problems, [9], [10] have demonstrated that the current BESO method can be extended to other constraints such as displacement. However it has never been developed to use fatigue as a constraint. In this paper, we introduce a fatigue-based topology optimization in the framework of the BESO. Our problem is formulated to minimize the volume if an object is subjected to a fatigue constraint. It is possible to perform the fatigue analysis and topology optimization in two separate steps, as presented in [11]; we can find the critical fatigue stress based on the specific life time and then use this stress as a constraint in our topology optimization problem.

There are three significant challenges that need to be overcome to effectively solve stress-based optimization problems [12]. The first one is related to the so-called “singularity” phenomenon [13]-[15], the second one is related to the local nature of the constraint, and the last one is related to the highly non-linear stress behavior. The “singularity” problem was first encountered when designing trusses subject to stress constraints, where it was shown that the n-dimensional feasible design space contains degenerate subspaces of dimension less than n [16], [13]. In the BESO approach, two phases, typically representing void or solid material, are used and no singularity problem occurs because the stress constraint is only applied to the solid phase. The final design is also free from the intermediate design variable values between solid and void that remain for the continuous density formulation.

The second difficulty of stress-based topology optimization is due to the local nature of the stress constraint. A large number of failure criteria should be defined for every element in a sub-optimization problem which is difficult for a gradient-based optimizer to solve efficiently. To remedy this situation, a p-norm approach has been proposed which aggregates many local constraints into one global constraint. The last issue with the stress constraint is its highly nonlinear dependence on the design. According to [6], a highly non-linear stress constraint is often observed when relaxation techniques are employed to cope with the singularity issue. Consequently, the aforementioned challenges clearly highlight the complexity of obtaining global optima through stress-based topology optimization. After addressing these challenges, this paper discusses the recent advances making it possible to conduct the stress-based BESO method. Despite the drawbacks of the four nodes bilinear quadrilateral elements, see [17], it has been used in this paper due to its simplicity, low computational cost and its promising results as it has been used earlier in stress based problems in [7], [5].

II. Problem Formulation

Our aim is to minimize the volume subject to critical fatigue stress. The problem formulation reads:

Khodamorad Nabaki and Jianhu Shen are with the Centre for Innovative Structures and Materials, School of Engineering, RMIT University, GPO Box 2476, Melbourne, VIC 3001, Australia.
Xiaodong Huang is with the Faculty of Science, Engineering and Technology, Swinburne University of Technology, Hawthorn, Melbourne, VIC 3122, Australia (e-mail: xhuang@swin.edu.au).

$$(\mathrm{P})\begin{cases}\begin{cases}\min \sum_{i=1}^{N_i} V_i x_i = 0 \\ x_i = x_{\min} \text{ or } 1\end{cases} \\ s.t.\ \sigma_f^{PN}(x) \le \sigma_f^*\end{cases} \tag{1}$$

where $\sigma_f^{PN}(x)$ is a global modified P-norm based on maximum tensile principal stress which is discussed in Section III, V_i is the volume of an individual element .The binary design variable x_i denotes the density of ith element and a small value of e.g. 0.001 rather than 0 is used to denote the void elements. To evaluate the displacements, stress and other quantities, FE analysis is performed as follows:

$$\mathbf{KU} = \mathbf{F} \tag{2}$$

where $\mathbf{K}$ and $\mathbf{U}$ are the global stiffness matrix of the structure and displacement vectors. According to the SIMP model, the material interpolation scheme can be expressed as:

$$E(x_i) = E^0 x_i^{\,q} \tag{3}$$

where E^0 denotes the Young's modulus for solid material, q is the penalty exponent and in this paper is fixed as 3 unless stated. It is assumed that the Poisson's ratio is independent from the design variables and the stiffness matrix $\mathbf{K}$ can be expressed by the elemental stiffness matrix and design variables.

$$\mathbf{K} = \sum_i x_i^{\,q}\, \mathbf{K}_i^0 \tag{4}$$

where $\mathbf{K}_i^0$ denotes the elemental stiffness matrix for solid element.

III. Critical Fatigue Stress Measurement

In this section, we discuss the fatigue stress measure used in this paper. We use the global approaches [11] by using the modified P-norm to calculate a single fatigue stress measure from element stress evaluation points which are in the centroid of each element. Since fatigue failure occurs for compressive stress, the maximum tensile principal stress of elements contributes to the fatigue stress measurement. The P-norm stress is defined as:

$$\sigma_f^{PN}(x) = \left(\frac{1}{N_i}\sum_{i=1}^{N_i}(\sigma_a^1(x))^P\right)^{\frac{1}{P}} \tag{5}$$

where p is the P-norm factor, N_i is the number of stress evaluation points and σ_a^1 is the maximum tensile principal stress. Thus $\sigma_a^1 = \max(\lambda^1, 0)$, where $\lambda^1 > \lambda^2 > \lambda^3$ are the eigenvalues of the stress tensor:

$$S = \begin{bmatrix} S_{11} & S_{12} & S_{13} \\ S_{12} & S_{22} & S_{23} \\ S_{13} & S_{23} & S_{33} \end{bmatrix} \tag{6}$$

Increasing the value of the exponent p in (5) brings the P-norm value closer to the maximum stress. On the other extreme, p=1 will lead to mean stress calculation. Different p-values are evaluated in [7]. In principal it should be infinite, but in practice a value from 3 to 4 was reported by some authors to work properly. In this paper our numerical experiences show that a value from 3 to 5 works well.

IV. Critical Fatigue Stress

We can perform the fatigue analysis and the topology optimization in two separate steps [11]. We use the high cycle fatigue approach with constant proportional external load to calculate the critical fatigue stress. First, we seek the highest stress value that satisfies the Modified Goodman fatigue criteria:

$$\left(\frac{\sigma_a}{S_n} + \frac{\sigma_m}{S_u} = 1\right) \tag{7}$$

where σ_a, σ_m, S_n and S_u are alternating stress , mean stress, fatigue strength, and ultimate tensile stress of materials respectively. Using the Basquin law we can find the stress amplitude for the desired constant life. By substituting this stress amplitude as fatigue strength in Modified-Goodman equation we obtain a threshold criterion for fatigue failure according to the desired constant life. In the next step by calculating the alternating and mean stress of all elements we can find the maximum stress which satisfies the threshold criterion of fatigue failure. The critical fatigue stress calculation problem ($\mathrm{P_{crit}}$) only needs to be solved once during the optimization process. The problem reads:

$$(\mathrm{P_{crit}})\begin{cases}\max\ \sigma_f^* \\ s.t.\ \dfrac{\sigma_a}{S_n} + \dfrac{\sigma_m}{S_u} \le 1\end{cases} \tag{8}$$

According to the Modified-Goodman fatigue criterion, Fig. 1, to avoid fatigue failure, all combinations of the mean and alternating stress must lie under the Goodman-line (Safe Zone).

V. Sensitivity Analysis

The gradient of the modified P-norm stress in (5), is derived from the chain rule,

$$\frac{\partial \sigma_f^{PN}(x)}{\partial x_i} = \frac{\partial \sigma_f^{PN}(x)}{\partial \sigma_a^1} \frac{\partial \sigma_a^1(x)}{\partial x_i} \tag{9}$$

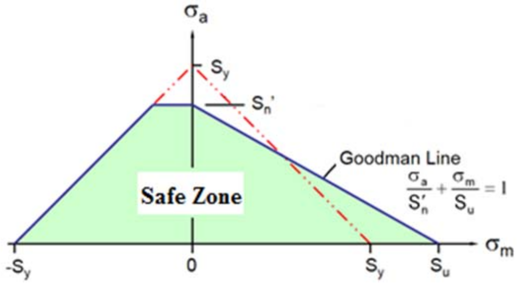

Fig. 1 Modified Goodman fatigue failure criterion

By taking the derivative of (5), the term $\frac{\partial \sigma_f^{PN}(x)}{\partial \sigma_a^1}$ can be calculated as:

$$\frac{\partial \sigma_f^{PN}(x)}{\partial \sigma_a^1} = \left(\frac{1}{N_i} \sum_{i=1}^{N_i} (\sigma_a^1(x))^P \right)^{\left(\frac{1}{P}-1\right)} \times \frac{1}{N_i} \left(\sigma_a^1(x) \right)^{P-1} \tag{10}$$

The derivative of the principal tensile stress vector in (9) with respect to design variable x_i gives.

$$\frac{\partial \sigma_a^1(x)}{\partial x_i} = \phi_i \frac{\partial S_{ij}}{\partial x_i} \phi_j = \mathbf{\Lambda}_t \frac{\partial \sigma_t}{\partial x_i} = \mathbf{\Lambda}_a \frac{\partial \boldsymbol{\sigma}_a(x)}{\partial x_i} \tag{11}$$

$$\mathbf{\Lambda} = (\phi_1^{\ 2}, \phi_2^{\ 2}, \phi_3^{\ 2}, 2\phi_1\phi_2, 2\phi_2\phi_3, 2\phi_1\phi_3)^T \tag{12}$$

$$\frac{\partial \boldsymbol{\sigma}_a(x)}{\partial x_i} = \frac{\partial \mathbf{D}(x)}{\partial x_i} \mathbf{Bu} + \mathbf{DB} \frac{\partial \mathbf{u}(x)}{\partial x_i} \tag{13}$$

where ϕ_i is the component of corresponding eigenvector and $\mathbf{D}$, $\mathbf{B}$ and $\mathbf{u}$ are the constitutive matrix, the strain displacement matrix corresponding to stress evaluation point of ith element and displacement matrix respectively. The term $\frac{\partial \mathbf{u}(x)}{\partial x_i}$ in (13) is calculated from the global state (2). By considering the chain rule we get:

$$\frac{\partial \mathbf{F}}{\partial x_i} = \frac{\partial \mathbf{K}(x)}{\partial x_i} \mathbf{u} + \mathbf{K} \frac{\partial \mathbf{u}(x)}{\partial x_i} \tag{14}$$

From which the $\frac{\partial \mathbf{u}(x)}{\partial x_i}$ can be calculated as:

$$\frac{\partial \mathbf{u}(x)}{\partial x_i} = -\mathbf{K}^{-1} \frac{\partial \mathbf{K}(x)}{\partial x_i} \mathbf{u} \tag{15}$$

Substituting (15) into (13) and then (13) into (11) and finally (11) into (9) gives:

$$\frac{\partial \sigma_f^{PN}(x)}{\partial x_i} = \frac{\partial \sigma_f^{PN}(x)}{\partial \sigma_a^1} \times \mathbf{\Lambda}_a \left(\frac{\partial \mathbf{D}(x)}{\partial x_i} \mathbf{Bu} - \mathbf{DBK}^{-1} \frac{\partial \mathbf{K}(x)}{\partial x_i} \mathbf{u} \right) \tag{16}$$

Considering the adjoint method we can define the adjoint equation by:

$$\mathbf{K}\boldsymbol{\lambda}^T = \mathbf{B}^T \mathbf{D}^T \mathbf{\Lambda}_a \frac{\partial \sigma_f^{PN}(x)}{\partial \sigma_a^1} \tag{17}$$

By inserting the adjoint variable into (9), the final gradient reads:

$$\frac{\partial \sigma_G^{PN}(x)}{\partial x_i} = \left[\frac{\partial \sigma_G^{PN}(x)}{\partial \sigma_a^1} \mathbf{\Lambda}_a^{\ T} \frac{\partial \mathbf{D}(x)}{\partial x_i} \mathbf{Bu} - \boldsymbol{\lambda}^T \left(\frac{\partial \mathbf{K}(x)}{\partial x_i} \mathbf{u} \right) \right] \tag{18}$$

VI. BESO Procedure

The evolutionary iteration procedure can be outlined as follows:

Step 1: Discretize the whole design domain using a finite element mesh.

Step 2: Define the BESO and stress calculation parameters such as evolutionary ratio ER, penalty exponent q, and p-normal exponent p.

Step 3: Carry out finite element analysis (FEA) for the real structure and virtual structure (the structure undergoes the dummy load) using FEA MATLAB code in this manuscript. Then output the data for calculating the sensitivity numbers based on the tensile principal stress.

Step 4: Determine the target volume for the next design based on the p-norm fatigue stress and critical fatigue stress constraint.

Step 5: Filter sensitivity numbers in the whole design domain by:

$$\hat{\alpha}_i = \frac{\sum_{j=1}^{N} w(r_{ij}) \alpha_i}{\sum_{j=1}^{M} w(r_{ij})} \tag{19}$$

where r_{ij} denotes the distance between the center of the element i and element j. $w(r_{ij})$ is the weight factor given as

$$w(r_{ij}) = \begin{cases} r_{\min} - r_{ij} & \text{for } r_{ij} < r_{\min} \\ 0 & \text{for } r_{ij} \geq r_{\min} \end{cases} \tag{20}$$

where $r_{\min}$ is the filter radius. Due to the discrete design variable used in the BESO algorithm, [18]-[21] proposed that the elemental sensitivity number can be further modified by averaging with its historical information to improve the convergence of the solution. That is, the sensitivity number after the first iteration is calculated by:

$$\tilde{\alpha}_i = \frac{1}{2}(\hat{\alpha}_{i,k} + \hat{\alpha}_{i,k-1}) \tag{21}$$

where k is the current iteration number. Then let $\hat{\alpha}_{i,k} = \hat{\alpha}_i$ which will be used for the next iteration, thus, the modified sensitivity number considers the sensitivity information in the previous iterations.

Step 6: Reset the design variables of all elements. For solid elements, the elemental density is switched from 1 to $x_{\min}$ if the following criterion is satisfied.

$$\alpha_i \leq \alpha_{th} \tag{22}$$

For void elements, the elemental density is switched from $x_{\min}$ to 1 if the following criterion is satisfied

$$\alpha_i > \alpha_{th} \tag{23}$$

where $\tilde{\alpha}_{th}$ is the threshold of the sensitivity number which is determined the relative ranking of the sensitivity numbers. The details about the calculation of $\tilde{\alpha}_{th}$ may refer to [20].

Step 8: Repeat 3–7 until the solution is convergent.

VII. Examples

To show the validity of the present fatigue-based topology optimization in the frame work of BESO method, this section provides optimal layouts for the L-shape beam with a fixed upper edge. This is the most popular example of stress based topology optimization and has been considered in much previous research; see [7], [3], [6], [4], [22].

The dimensions of the L-beam are seen in Fig. 2, where the domain is meshed with 6400 equal sized four node elements. Fig. 3 shows the Goodman fatigue diagram for the case of fatigue optimization (1.0 mm by 1.0 mm) and the thickness of the structure is 1 mm. The material is carbon steel 1018 and with material data; Young's modulus 210,000 MPa, Poisson's ratio 0.3 and yield limit and S_u are 358 MPa and 440 MPa, respectively. Magnitudes of the mean and 1 Hz alternating forces were set to 250 N and 450 N, respectively; it should be emphasized that the forces are constant proportional loadings. The exponent of the Basquin equation, b, were set -0.0851. The minimum desired number of loading cycles for the S-N curve, N_f, was set to 10^7 from which we can calculate the fatigue stress S_n that is180.82 Mpa. Finally, by considering the modified- Goodman fatigue failure and the combination of the mean and alternating stress the critical fatigue stress for 10^7 cycles obtained as 337.62 Mpa which has been used as stress constraint in the example. 3 × 2 numbers of elements under the load have been excluded from the design space to avoid stress concentration under applied load. The sensitivity filter is applied with a filter radius, rmin = 1.5 mm.

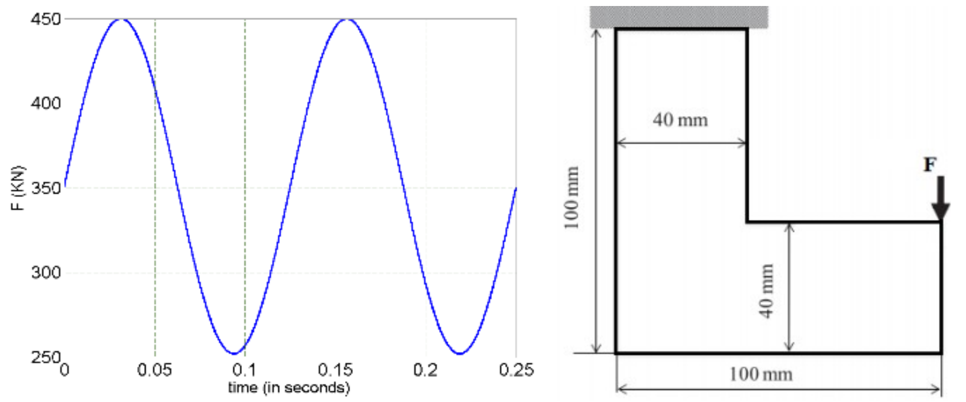

Fig. 2 Design domain, loading and boundary conditions of the L-beam

Solution for the L-beam problem for fatigue optimization and compliance can be found in Tables I and II. In the case of fatigue optimization we minimize the volume based on the critical fatigue stress however in the case of compliance minimization to compare the result with fatigue case we set the volume constraint equal to the optimized volume which we obtained in the fatigue case (v/v_0=0.421).

In the case of compliance minimization, we have large stress concentration, and as it can be seen from Fig. 5, the combination of the mean and alternating stresses are not in the safe zone and the fatigue failure will occur before the prescribed life cycles. However, the stress distribution of elements in the case of fatigue optimization is more uniform than the compliance method, and as it has shown in Fig. 3, the scatter of the mean and alternating stresses lies in the safe zone and fatigue failure will not occur. Fig. 4 shows the convergence plot of the fatigue optimization problem. We have considered the uniaxial stress state for calculation of the critical fatigue stress by the Modified- Goodman fatigue failure criterion.

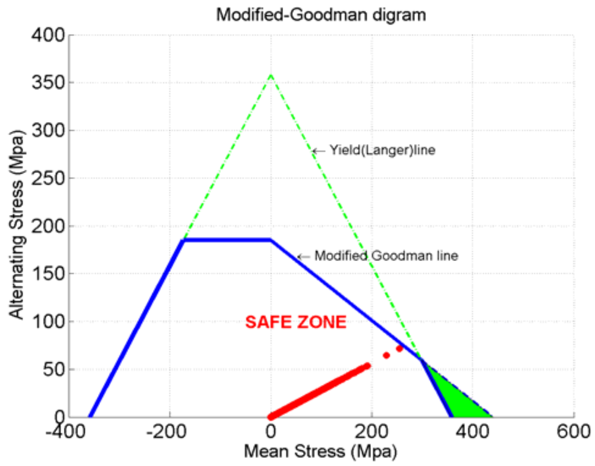

Fig. 3 Goodman fatigue diagram used in the fatigue optimization

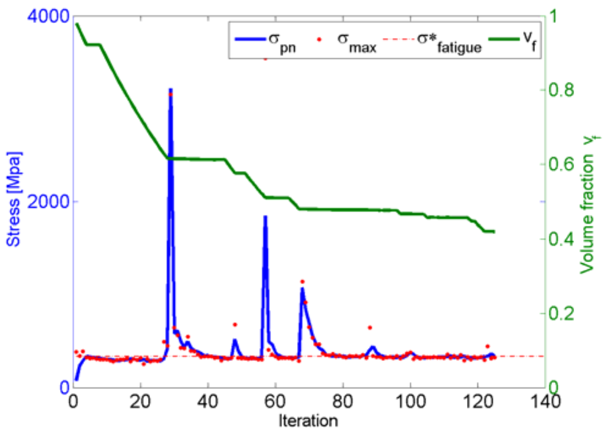

Fig. 4 Convergence plot for the case of fatigue optimization

TABLE I
FATIGUE-BASED BESO LAYOUTS FOR L-BRACKET

Optimized Structure	
Tensile principal Stress plot [MPa]	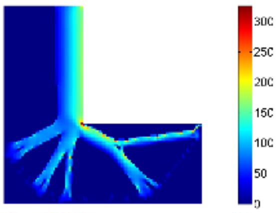
von Mises Stress Plot [MPa]	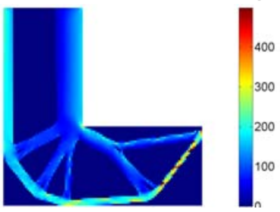
v/v_0	0.421
c [N mm]	249.521

TABLE II
COMPLIANCE-BASED BESO LAYOUTS FOR L-BRACKET

Optimized Structure	
Tensile principal Stress plot [MPa]	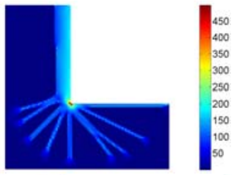
von Mises Stress Plot [MPa]	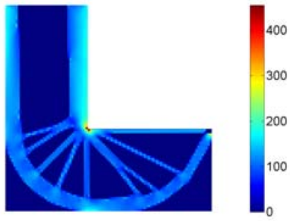
v/v_0	0.421
c [N mm]	189.423

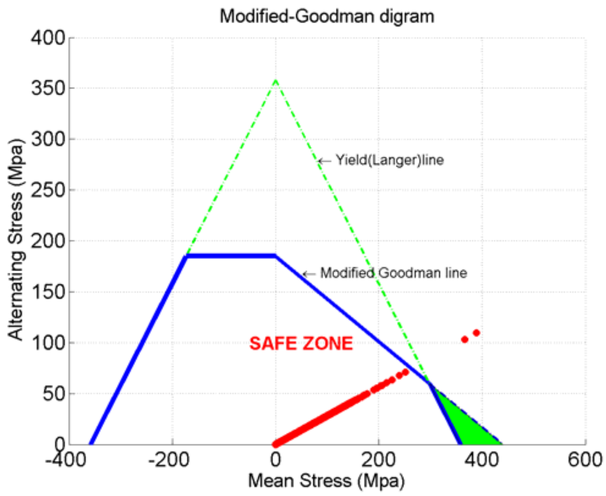

Fig. 5 Goodman fatigue diagram for compliance case

VIII. CONCLUSIONS

Since fatigue failure is one of the most important criteria for engineering problems and it has never been developed in the BESO method, in this paper, we proposed the BESO method for the high cycle fatigue optimization by considering the maximum tensile principal stress and modified Goodman fatigue failure criterion. The method has been verified numerically and the obtaining results are appealing. Compared with the traditional compliance minimization problem where fatigue failure may occur, the numerical example shows that considering critical fatigue stress in the BESO method allows for designs of a practical engineering structure free from fatigue failure for prescribed life cycles.

References

[1] Bendsøe, M. P. and N. Kikuchi, *Generating optimal topologies in structural design using a homogenization method.* Computer methods in applied mechanics and engineering, 1988. 71(2): pp. 197-224.

[2] Svanberg, K., *The method of moving asymptotes—a new method for structural optimization.* International journal for numerical methods in engineering, 1987. 24(2): pp. 359-373.

[3] Bruggi, M. and P. Duysinx, *Topology optimization for minimum weight with compliance and stress constraints.* Struct Multidisc Optim, 2012. 46(3): pp. 369-384.

[4] Holmberg, E., B. Torstenfelt, and A. Klarbring, *Stress constrained topology optimization.* Struct Multidisc Optim, 2013. 48(1): pp. 33-47.

[5] Jeong, S. H., D.-H. Choi, and G. H. Yoon, *Separable stress interpolation scheme for stress-based topology optimization with multiple homogenous materials.* Finite Elements in Analysis & Design, 2014. 82: pp. 16-31.

[6] Jeong, S. H., et al., *Topology optimization considering static failure theories for ductile and brittle materials.* Computers and Structures, 2012. 110-111: pp. 116-132.

[7] Le, C., et al., *Stress- based topology optimization for continua.* Struct Multidisc Optim, 2010. 41(4): pp. 605-620.

[8] París, J., et al., *Stress constraints sensitivity analysis in structural topology optimization.* Computer Methods in Applied Mechanics and Engineering, 2010. 199(33): pp. 2110-2122.

[9] Huang, X. and Y. M. Xie, *Convergent and mesh-independent solutions for the bi-directional evolutionary structural optimization method.* Finite Elements in Analysis & Design, 2007. 43(14): pp. 1039-1049.

[10] Rozvany, G. I. N., *A critical review of established methods of structural topology optimization.* Structural and Multidisciplinary Optimization, 2009. 37(3): pp. 217-237.

[11] Holmberg, E., B. Torstenfelt, and A. Klarbring, *Fatigue constrained topology optimization.* Structural and Multidisciplinary Optimization, 2014. 50(2): pp. 207-219.

[12] Bendsøe, M. P., *Topology Optimization: Theory, Methods, and Applications*, ed. O. Sigmund. 2004, Berlin/Heidelberg: Berlin/Heidelberg : Springer Berlin Heidelberg.

[13] Cheng, G. and Z. Jiang, *Study On Topology Optimization With Stress Constraints.* Engineering Optimization, 1992. 20(2): pp. 129-148.

[14] Cheng, G. and X. Guo, *ε-relaxed approach in structural topology optimization.* Structural Optimization, 1997. 13(4): pp. 258-266.

[15] Rozvany, G. I. N., *On design-dependent constraints and singular topologies.* Struct Multidisc Optim, 2001. 21(2): pp. 164-172.

[16] Kirsch, U., *On singular topologies in optimum structural design.* Structural Optimization, 1990. 2(3): pp. 133-142.

[17] Cook, R. D., *Concepts and applications of finite element analysis*. 4th ed. ed, ed. R. D. Cook. 2001, New York: Wiley.

[18] Huang, X. and Y. Xie, *Convergent and mesh-independent solutions for the bi-directional evolutionary structural optimization method.* 2007.

[19] Huang, X. and Y. Xie, *Evolutionary topology optimization of continuum structures with an additional displacement constraint.* Struct Multidisc Optim, 2010. 40(1): pp. 409-416.

[20] Huang, X. and Y. Xie, *Evolutionary topology optimization of geometrically and materially nonlinear structures under prescribed design load.* Structural Engineering and Mechanics 2010. 34(5): pp. 581-595.

[21] Yi, J., et al., *A topology optimization method for multiple load cases and constraints based on element independent nodal density.* Structural Engineering and Mechanics, 2013. 6(45): pp. 759-777.

[22] Jensen, K. E., *Solving stress and compliance constrained volume minimization using anisotropic mesh adaptation, the method of moving asymptotes and a global p-norm.* Structural and Multidisciplinary Optimization, 2016. 54(4): pp. 831-841.